International Forum on Aeroelasticity and Structural Dynamics
IFASD 2019
10-13 June, Savannah, Georgia, USA

EXPERIMENTAL AND NUMERICAL IMPLEMENTATION OF ROBUST CONTROL FOR ATTENUATION OF BUFFET LOADS

Sheharyar Malik[1], Sergio Ricci[2], Luca Riccobene[2] and Daniele Monti[3]

[1]Department of Aerospace Engineering Technology,
Abu Dhabi Polytechnic, IAT, United Arab Emirates.
sheharyar.malik@adpoly.ac.ae

[2]Department of Aerospace Science and Technology,
Politecnico di Milano, 20156 Milano, Italy.
sergio.ricci@polimi.it

[2]Department of Aerospace Science and Technology,
Politecnico di Milano, 20156 Milano, Italy.
luca.riccobene@polimi.it

LEONARDO Company, Aircraft Division,
Venegono Inferiore, VA, Italy.
daniele.monti@leonardocompany.com

Keywords: Robust control, aeroelastic, slender wing, experimental validation, attenuation.

Abstract: This paper presents a robust control design for aerodynamically efficient slender wing. Incoming flow and buffet loads can easily excite the aeroelastic modes of the slender wings. A schematic design procedure based on infinity norm presents a way to attenuate the excited modes of the wing. It facilitates the robustness of the system even in the absence of high-fidelity structural and aerodynamic model. Multi Input Multi Output (MIMO), Linear Time Invariant (LTI) aeroelastic state-space system representing the multiple control surfaces and sensors of X-DIA wing forms the base of this research. Novel technique transfers a system from Multi Input Multi Output (MIMO) to Single Input Single Output (SISO) aeroelastic state-space system. Moreover, using the complexity of aeroelastic system to our advantage, mode selection reduces the order of the state space model, as a prerequisite to avoid higher order of a robust controller. The results of the reduced order model matched precisely with the full state model. Real Time Application Interface (RTAI) performs data acquisition to implement the robust control scheme in the wind tunnel tests. The test campaign validates the numerical implementation of robust control law. The developed robust control scheme added damping and attenuated the first bending mode significantly. Frequency response is presented to illustrate the results for both numerical and experimental results.

1 INTRODUCTION

Aeroelastic systems combines the structural model, aerodynamic model and their adverse interaction. These models are idealization of real world aeroelastic phenomenon. The phenomenon is complicated enough that even high fidelity models come with approximations, and uncertainties are associated with it. It increases the need of control system that performs robustly for uncertain conditions. This underlines the importance of robust controllers for aeroelastic systems as they take the uncertainties by default in the state space models. Traditional control with optimal solution and Linear Quadratic Gaussian (LQG) finds a solution for nominal system while the robust controller can give a solution for worst case system with uncertainties. In addition, it also confines the active control system with in a specific frequency range [1, 2].

Since its formulation in 1991, H-infinity method has provided the base to robust control techniques for different application [3]. Analytically, H-infinity methods and robust control has now become a mature field that involves diverse techniques of analysis in presence of uncertainties to alleviate or minimize the disturbance. However, practical achievements of robust control are rare as compared to the other classical control techniques. It is reported that robust controllers encounters two sets of problems. First problem originates when the real world problems are represented by state space model, the order of the model is high and secondly their application to the real world, as these controllers usually suffer the insufficiency of the system compatibility to meet the controller requirement, especially for the case of Mu synthesis where the order of the controller exceeds the order of plant. H-infinity and Mu controller are implemented in the real time for the linear time invariant state space model of 4^{th} order with two inputs and two outputs. H-infinity controller ensured efficient attenuation of disturbances. Mu-controller ensured robust performance in the presence of parametric uncertainties. The resulting h-infinity controller order is of same order as the order of the plant [4].

State space h-infinity solutions are derived for Linear Time Invariant (LTI) models [5]. A thorough analysis of these techniques is given in [6, 7], the research also suggested the output feedback by employing a dynamic controller. It is well known that performance of controller based on infinity norm is better than controller based on H_2 optimal controller. Recently, robust control techniques are implemented for robust stability of active aeroelastic wing and space launch vehicle [8, 9]. NASA Dryden has recently implemented their robust control system for X-56 aircraft [10]. Active control based on h-infinity technique takes notice of structural velocity, acceleration as the output feedback and employ actuators to achieve vibration suppression, this approach has been successfully used in defining globally robust controller for aeroelastic wing [11]. Recently, a robust controller is designed for flutter suppression. The mini MUTT (Multi Utility Technology Testbed) aircraft, has high aspect ratio wing which compromises on structural stiffness, therefore flutter speed is reduced and operational speed is limited. A schematic design procedure for h-infinity control is presented in [12].

Advanced wings that employ multiple control surfaces are used to enhance their aeroelastic response under the projects of NASA Active Flexible Wing (A.F.W.) and Active Aeroelastic Wing [13, 14]. The availability of the multi surface analysis gives the freedom of multitasking and a dedicated control surface can be used for structural mode attenuation.

This research presents an application of active robust control on already available aeroelastic wing of X-DIA aircraft. X-DIA is an unconventional forward swept wing with the availability of multiple control surfaces and sensors. The difficulties posed in the formulation of robust controller are addressed by the newly developed model order reduction techniques. The research uses the comparison of model reduction techniques to reduce the order of the system. It also highlights the selection criteria for using single control surface and sensor for the robust control. The computational difficulty of real time data acquisition is solved by MATLAB/RTAI where the dynamic controller is implemented in the real time environment.

The following sections presents the geometrical features of the X-DIA wing and its state space model synthesis. Numerical implementation of robust control is presented in section 4, it includes the system model along with time delay, phase delay and formulation of active control law. The section will outline the h-infinity method followed by tuning of the control law. Section 5 shows the experimental setup and activity conducted for validation followed by conclusions.

2 X-DIA WING MODEL

The section presents the nomenclature of X-DIA wing and formulation of its corresponding state space model. The wing was built as a result of collaboration between Politecnico di Milano (POLIMI) under European project Active Aeroelastic Aircraft Structures (3AS). It is a scaled down model of original wing for regional commercial aircraft X-DIA. The aircraft is unconventional and it provides innovative solution to fuel-efficient flight [15, 16]. Prototype of X-DIA has been effectively used for structural and aerodynamic research outcomes [17].

As shown in figure 1, the wing is equipped with four control surfaces to deal with the flexible modes of the wing in addition to flight mechanics of the aircraft. Two control surfaces are situated on the leading edge, named as leading-edge outboard (LEO) and leading-edge inboard (LEI). Similarly, two control surfaces are present at the trailing edge of the wing, named as trailing edge outboard (TEO) and trailing edge inboard (TEI). Moreover, single elastic spar supports the structure of the wing.

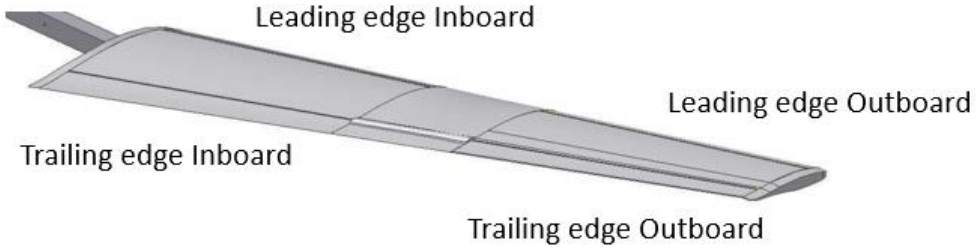

Figure 1: X-DIA Wing

The wing is equipped with four PCB monoaxial accelerometers placed adjacent to the control surfaces by obeying the identically located acceleration and force (ILAF) law. The PCB monoaxial accelerometers have bandwidth of 3 kHz. Wing-tip acceleration is extracted by the virtue of two wing tip accelerometers located near the leading edge outboard and trailing edge outboard. The accelerations at the wingtip are added to get the average of bending mode and subtracted to extract the average of torsional mode. The accelerations are processed by Power Spectral Density (PSD) and Frequency Response (FR) to highlight the appearance of first bending mode and first torsion mode. The electric motors that drives the four control surfaces

(LEI, LEO, TEI and TEO) are selected by fulfilling the criteria set by physical design constraints such as weight and maximum allowable size of the motors. Comparative study of static and dynamic characteristics showed that the ideal motors for the X-DIA wing are Portescap mod 17N78-210E. Each motor is also equipped with encoder. Thanks to planetary gears in shaft/line torque transmission, chief concern of torque and gear reduction are met. The schematic of the wing is shown in figure 2.

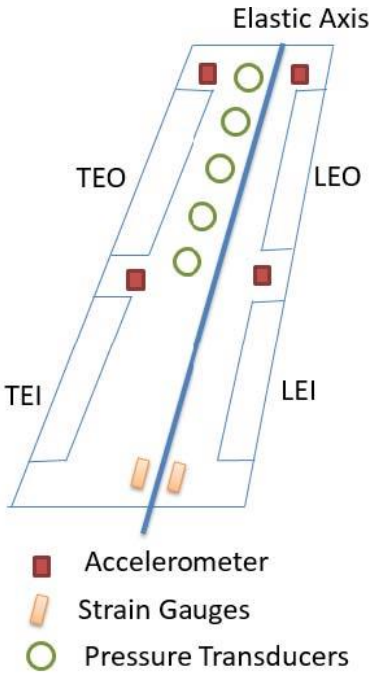

Figure 2: Schematic of X-DIA wing

3 STATE SPACE MODEL

Low and higher order models can be built with compromise on fidelity level to predict the excited modes. Aeroelastic phenomena can be grasped with high fidelity by Linear Time Invariant (LTI) state space models [18]. Commercially available software MSC/NASTRAN is used to couple the structural model and aerodynamic model based on Doublet Lattice Method (DLM). Mass, damping and stiffness matrices extracted from the dynamic aeroelastic analysis are casted by the help of the in-house developed software MASSA to form the multi-input multi-output state space system. Complete time domain aeroelastic model can be furnished by selecting appropriate structural outputs for feedback along with aerodynamic and actuator inputs. The created state space model has 13 Inputs and 8 outputs, with 108 states. Five inputs are defined for five piezo resistive patches that are attached on the upper surface of the wing to extract the external dynamic loads due to buffet phenomenon. Four inputs are defined for external forces on exactly the same grid points where accelerometers are placed. Lastly, four inputs are provided for the four control surfaces that provides the control over the structural dynamics of the wing. Four outputs are defined for four structural accelerations corresponding to the four accelerometers attached on the wing. It is user dependent to extract structural velocities and displacements depending upon the performance and feedback requirement of the system. Four outputs are allocated for the rotation of control surfaces associated with active control. The generic diagram of the state space model is shown in the following figure 3.

The behaviour of the wing is observed for different speeds ranging from 20, 30, 40 m/s. The amplitude of vibrations consistently increased along with shift in the excitation frequency with increase in the velocity.

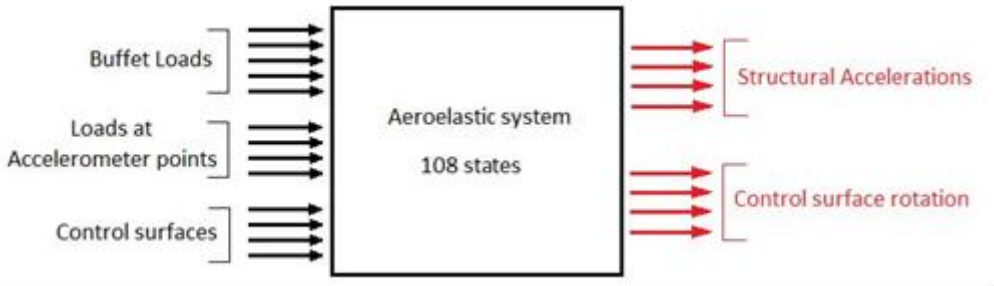

Figure 3: State space model (Multiple inputs and multiple outputs)

4 CONTROL SYSTEM FORMULATION

Numerical analysis formed the basis to perform the experimental validation, this section presents the dynamics of the instrumentation and wing model. For flight mechanics control, the bandwidth of actuator and sensors is negligible as compared to the closed loop bandwidth of active control system designed for flutter suppression and attenuation of vibrations. In addition, for flight mechanics the sampling rate of the signal is higher than the active control system. Thus, the bandwidth of actuator and sensor are of huge importance when the objective is to attenuate vibrations and unstable flutter etc. Actuator and sensor models are separately designed owing to the availability of actuator and sensor in the wind tunnel laboratory at Politecnico di Milano. The electric motors have bandwidth of approximately 30 Hz. The bandwidth of actuators is tested by the method detailed in [17], the effectiveness of actuator is assessed in frequency domain and time domain by chip signal and step signal, respectively. The actuators dynamics is modelled by second order low pass filters and given as G_{act} in eq. 1:

$$G_{act} = \frac{\omega_o^2}{s^2 + 2\xi_o\omega_o s + \omega_o^2} \tag{1}$$

The model will incorporate the phase loss and thus it is one way of introducing delay in the system. The signals provided by the sensors are the processed by PCI boards and then they are passed to actuators. The slow dynamics of actuators as compared to sensors are ignored and sensor dynamics is incorporated in the main model. Time delays introduced by digitalization of electrical signals often leads researchers to trade-off between continuous and discrete signals. Continuous time signals demands for the time delay to be included in the model along with digitalization. On the contrary, the discrete time based design will automatically incorporate the time delay in the system. So, based on the available setup, discrete system is opted for real time data acquisition.

Robust control scheme is developed owing to the beneficial features offered by the multi-surface wing of the X-DIA aircraft. The geometrical features of the wing eases this task and offers many possibilities, as one sensor and one actuator is selected to simulate the input and output behaviour of the state space model. Comparative study is performed on X-DIA wing based on Hankel singular values and frequency response [2]. The study leads to the selection of suitable control surface to attenuate the specific excited mode, the system is reduced to

(SISO) single input single output, trailing edge outboard actuator and trailing edge outboard accelerometer. However, the choice to switch between different outputs and inputs is in-hand and can be altered.

For H_∞ controller, every state of the model results in a state of the controller. The order of the plant is the prime concern. So, the model order reduction is achieved by two approaches. Balanced truncation computes a low order model by the use of Hankel singular Values (HSV), it preserves the dynamics of important state while discarding other states. The full order of the state space model comprised of 108 states is reduced to 50 states, it is reduced with the help of multiplicative error bound. Inbuilt MATLAB function, which uses balanced stochastic model truncation via Schur method based on multiplicative (relative) error bound to achieve the target. The benefit of using the method, is in the fact that for some systems with low damped poles or zeros, the balanced stochastic method produces a better reduced-order model fit in certain frequency ranges to make multiplicative error small. Whereas additive error methods only cares about minimizing the overall "absolute" peak error, they can produce a reduced-order model missing those low damped poles/zeros frequency regions. The comparison of full order system and reduced order system is shown in figure 4. The number of states of the system is not of prime importance as the developed controller is independent of number of states in the plant. The controller formed by this technique produces high order controller. This is challenging task for the controller to minimize the highest gain among high number of states and find a structural value for all inputs and outputs.

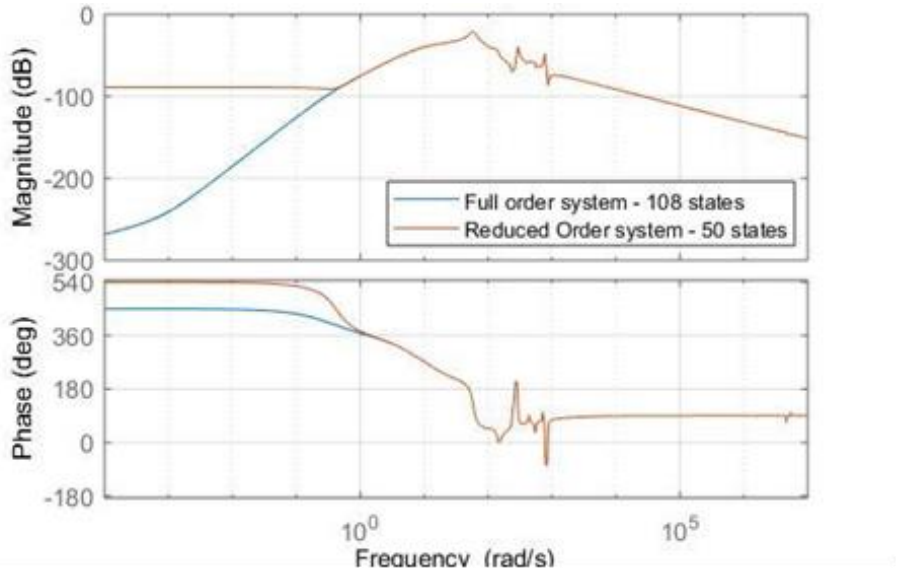

Figure 4: Balanced Truncation Method – reduced order

A novel concept based on the dynamical nature of the state space model is used. Specific modes of interests are selected. Model selection eliminates the modes and associated poles that are of no interest. The mode selection was also consistent with the allowable actuator dynamics and bandwidth. The result of the model order reduction is shown in figure 5.

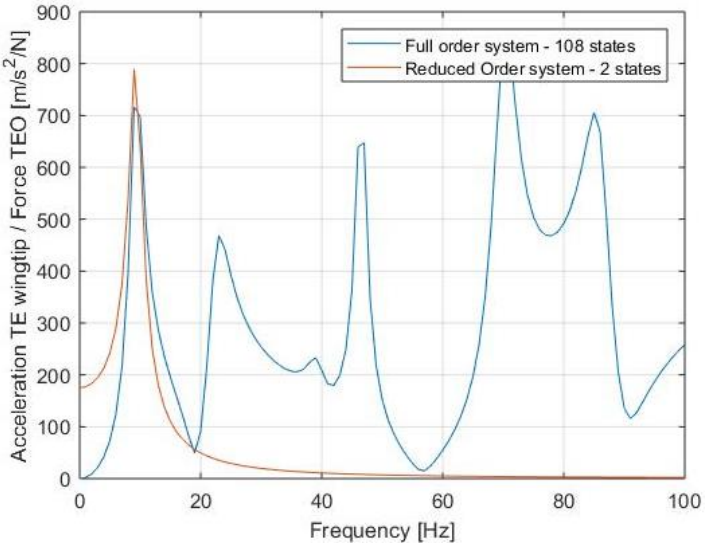

Figure 5: Comparison of Full and Reduced Order Systems

Robust control is a mature field analytically but rarely has it been used in experimentation or for practical purposes in a dedicated aeroelastic systems. The objective of the controller is to attenuate the vibrations. Also, it must provide robust stability and performance to wide range of uncertainties in the aeroelastic system by implementing dynamic robust controller based on approach like H-Infinity. The H_∞ (infinity norm) of Linear Time Invariant (LTI) system for input to output is given by:

$$\|G(s)\| = \sup_{\omega} \bar{\sigma}(G(j\omega)) \tag{2}$$

Where ' $\bar{\sigma}$ ' represents the largest singular value throughout the frequencies 'ω' of interest. The infinity norm measures the maximum gain or amplification of transfer function for all input and output directions. The measured h-infinity norm assessed the performance of the plant in a closed loop system. The purpose of the controller is to stabilize the closed loop by linear fractional transformation $F_l(P,K)$ that produces performances index 'γ' which provides an upper bound of the closed loop $\|F_l(P,K)\|_\infty$. The outcome of the synthesis is a dynamic controller as a result of solution to two Riccati equations. Once the meaningful performance specifications are defined for desired inputs and outputs then the synthesis is efficiently performed by Robust Toolbox, MATLAB. The control architecture is shown in figure 6:

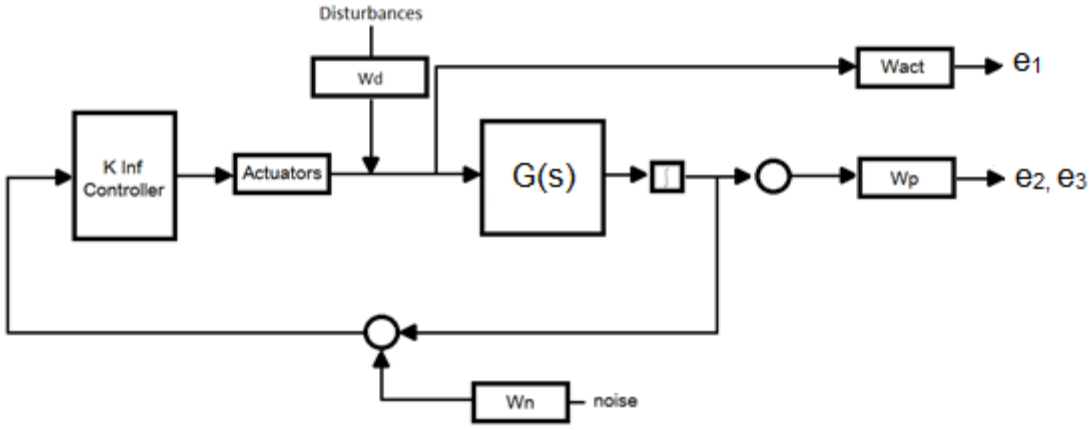

Figure 6: Control Scheme - Robust Controller

The plant model represent the airframe model along with instrumentation dynamics of the system. The measurable output y, is used for feedback and it consists of signals from accelerometers. The input to the plant is symmetrical deflection of trailing edge outboard. Where, blocks W_{act} and W_{pz} represents weighting functions on the actuator bandwidth and performance of the system, respectively. Outputs e_1, e_2, e_3 are the weighted version of control signals. Noise and disturbance are the exogenous inputs to the system weighted by W_d and W_n. These five signals complete the mapping for low fractional transformation and it can be represented by six transfer functions.

$$\begin{bmatrix} e_1 \\ e_2 \\ e_3 \end{bmatrix} = \begin{bmatrix} W_{act} & & \\ & W_{py} & \\ & & W_{pz} \end{bmatrix} \begin{bmatrix} -T_1 & S_1K \\ G_yS_1 & T_2 \\ G_zS_1 & G_zS_1K \end{bmatrix} \begin{bmatrix} W_d & \\ & W_n \end{bmatrix} \begin{bmatrix} \text{disturbance} \\ \text{noise} \end{bmatrix} \tag{3}$$

Input complementary and output complementary sensitivity are given by T_1 and T_2, respectively. Input sensitivity, disturbance sensitivity and control sensitivity are denoted by S_1, S_1K and G_yS_i, respectively. The weighting functions are selected based on the literature review and previous experimentations. The alteration is user defined, hence the weights are adjusted as per the importance of transfer functions. Control action can be enhanced by increasing the value of W_{act} while the damping and attenuation can be enhanced by increasing the values of W_{pz}.

Roll-out and wash-off frequencies are separated by large margin from the controller dynamics. It gives the freedom to design the inputs and outputs solely dependent on the controller requirements. Thus, W_{act} completely defines the dynamics of the controller as $S_1 = I$ and $T_i \approx 0$. The transfer function of performance output results in band pass filter. Performance and noise senstivity is shown in figure 7.

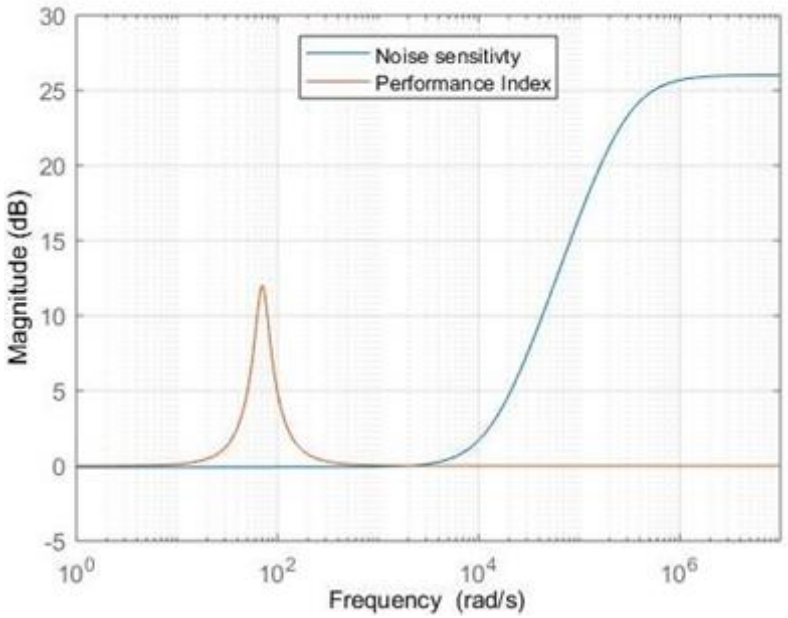

Figure 7: Noise and Performance Index

With all the weights removed, the loop is closed with a norm bounded stable LTI dynamic uncertainty $\Delta_i \in H_\infty$, such that noise = Δ_i e_1, disturbance = Δ_i e_1, the loop remains stable

according to small gain theorem, as long as $\|\Delta_i\| < 1/\|T_i\|$. The result for the open loop and closed system is shown in figure 8.

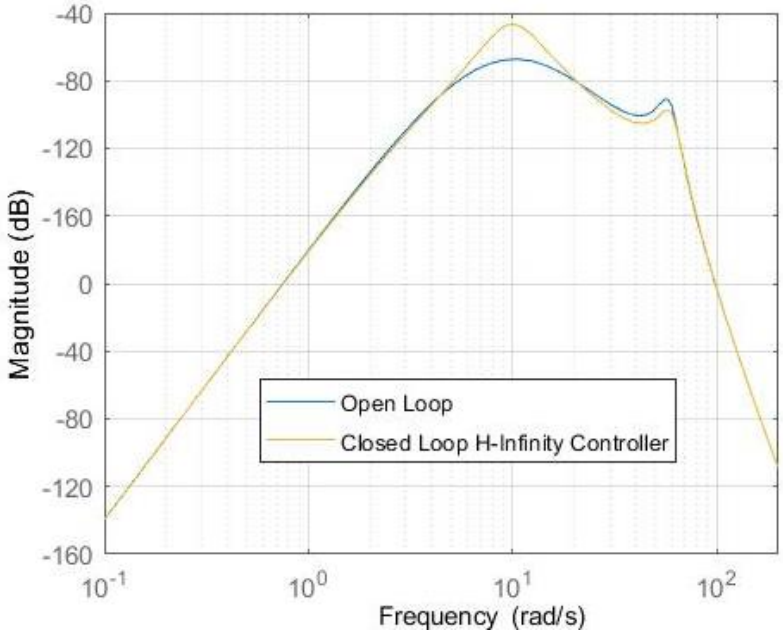

Figure 4: Frequency Response of Open and Closed Loop Systems

The advantage here lies in the fact that the controller is modelled with plant having uncertainties. frequency response is sued to demonstrate the effect of active control under H-infinity scheme. As the objective of this scheme was to attenuate the first bending mode, it is clear that the active control scheme not only attenuated the first bending mode but also provided additional damping. It is also worth mentioning that the closed loop has increased the magnitude at the neigboring frequencies that is the Inevitable consequence of bode sensitivity integral.

Aeroelastic system is made uncertain by introducing the parametric uncertainties in the state space matrix of the system. The uncertain system develops each performance output with respect to the amount of parametric uncertainty, the performance output deviates from the nominal (original) system output in terms of magnitude and phase. Nominal system is computed for certain system (without any uncertainty) along with samples comprised of different levels of uncertainties, worst case system is also computed for the provided uncertainty in the system. Three sets of uncertainty are introduced in the system, it includes uncertainty in the structural, aerodynamics and actuator system. The performance index $\|G_Z S_i\|/\|G_Z\|$ is calculated for the worst case H_∞-norm. The result is shown in figure 9. 20% of parametric uncertainty is introduced in the systems variable.

The robust stability and performance behaviour is directly related to the modelled uncertainty, System is robustly stable for 22% of modelled uncertainty. The system performs robustly for 17% of uncertainty in the state matrix of the aeroelastic system. 20 % of actuator uncertainty is separately introduced for actuator dynamics, norm bound multiplicative uncertainty on the actuator model.

Individual uncertainty is also tested against the stability and performance of the controller. Instability first occurred for aerodynamic system for 30% of parametric uncertainty that the

instability occurred for 40 % parametric uncertainty in the structural model. Keeping all the system nominal, the system performs robustly for 60 % of uncertainty in the actuator dynamics.

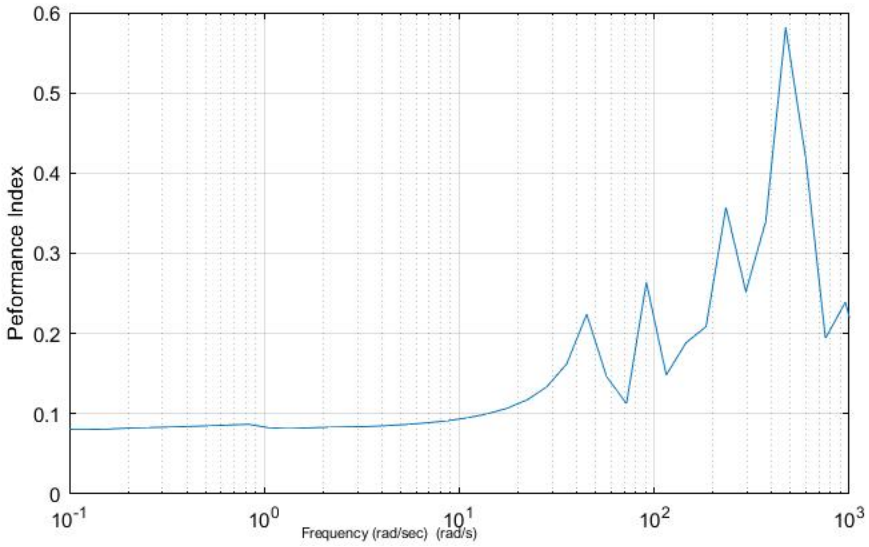

Figure 5: Structural singular Value

5 EXPERIMENTAL VALIDATION

The experimentation for active robust controller is performed at Department of Aerospace Science and Technology, Politecnico di Milano. A dedicated setup PC 3AS ALA is used to configure the wing in the wind tunnel. The wind tunnel has height of 1.5 m and width of 1 m with a wind speed limit of 55 m/s. By virtue of Special mounting system wing is placed in test section of the wind tunnel, it provides the wing the same constrained motion as when it is attached to the fuselage of the aircraft.

The setup PC 3AS ALA provided the connections between the sensors/actuators connected with the wing, input/output boards and Simulink model of the developed control scheme, is upgraded for experimental tests along with Linux operating system and up-to date versions of commercially available MATLAB/SIMULINK and RTAI Lab software are configured. The schematic of instrumentation is shown in figure 10.

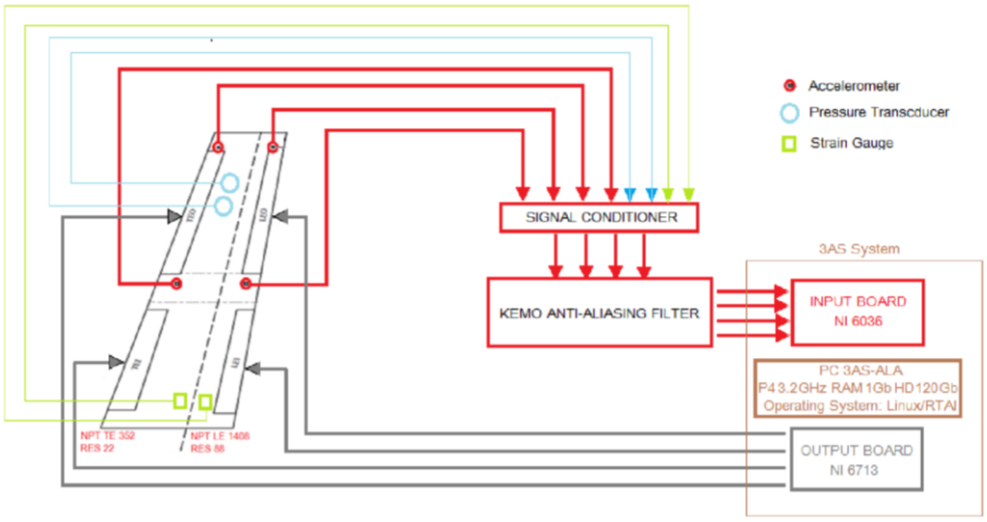

Figure 6: Connection of wing and PC 3AS ALA

Open source drivers are developed from Linux Control & Measurement Device Interface (COMEDI), for the plugin Input/output boards provided by National Instruments. These drivers are implemented as a core Linux 2.6 kernel module (distributed with COMEDI). Data acquisition for the wing is carried out with Real Time Application Interface for Linux (RTAI) 4.0. It develops the block diagrams that can be compiled and executed on the RTAI Linux operating system, it enables host and target systems to communicate with (establishes). XRTAI Lab provided the real-time events by providing graphic interface for gauges, scopes, meters and oscilloscopes etc. It also provided the ability to change the parameters for real time executable files. Signal conditioning for the sensors is performed by KEMO filters which also acted as anti-aliasing and noise reduction filters. Uncertainty is introduced in the gains of the system.

The closed loop frequency response has shown the attenuation for H-infinity controller with respect to the open loop response reduced state space system. The frequency response is shown in the figure 11.

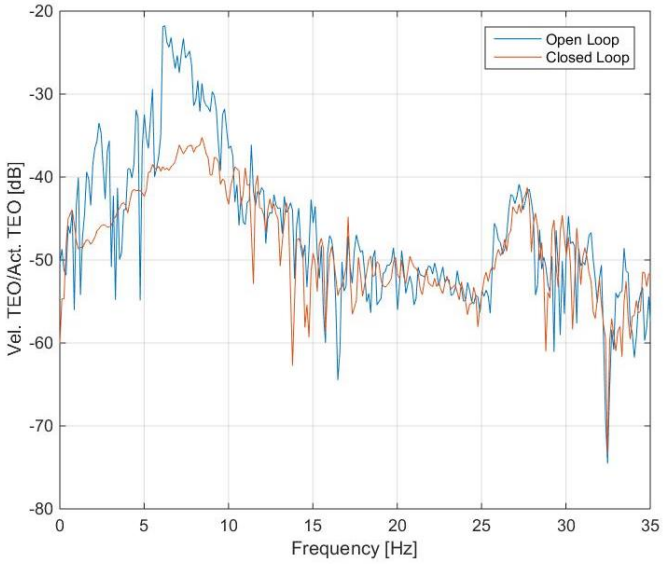

Figure 7: Frequency Response H-infinity Controller

The result is presented for first bending mode only as this was the targeted mode owing to the reduced state space model. The attenuation shown by robust controllers is relatively less as compared to the static output feedback controller due to the fact it is dealing with highly uncertain system, i.e. the robust controller is successful even dealing with worst possible case. The attenuation can be increased if the controller is relaxed by considering the less amount of uncertainty and changing the performance criteria for the system.

6 CONCLUSIONS

This paper presents numerical and experimental robust controller designed for the slender wing. The objective of the controller is to attenuate the vibrations associated with the first bending mode while keeping robust stability and performance under uncertainties. The control scheme is dedicated towards achieving globally robust control along with modelled actuator and sensor dynamics, in this context H-infinity controller is devised for the aeroelastic system. The aspect of model reduction procedure is successfully applied by decomposing the flexible body modes of the aeroelastic system. The reduced model retained its natural Linear Time Invariant (LTI) system behaviour over the range of frequencies in interest. The research also

illustrated the use of single control surface and single sensor to formulate the robust controller. The system attenuated the bending modes with additional damping and predicted the robust performance and stability of the reduced order aeroelastic system under uncertainties.

7 REFERENCES

[1] Fonte, F. Ricci, S. and Mantegazza, P. (2015). Gust Load Alleviation for a Regional Aircraft Through a Static Output Feedback, *Journal of Aircraft*, Vol. 52, No. 5, pp. 1559-1574.

[2] Malik, S. Riccobene, L. Ricci, S. And Monti, D. (2017). Development of a buffet load mitigation system based on multi surface control, *International Forum on aeroelasticity and structural dynamics*, Como, Italy.

[3] Zames, G. (1981). Feedback and Optimal Sensitivity: Model Reference Transformations, Multiplicative Semi Norms, and Approximate Inverses, *IEEE Transactions on Automatic Control*, Vol. 26, No. 2, pp. 301-320.

[4] Petkov, P., Slavov, T., Mollow, L., and Kra Lev, J. (2015). Real Time Implementation of H-Infinity and Mu Controllers, *Journal of Applied and computational mathematics*, Vol. 14, No. 1, pp. 87-100.

[5] Doyle, J. H., Glover, K., Khargonekar, P., and Francis, B. (1989). State Solutions to Standard H_2 and H_∞ Control Problems, *IEEE Transactions on Automatic Control*, 34(8), 831-847.

[6] Basar, T. P., and Bernard, P. (1991). H_∞ Optimal Control and Related Minimax Design Problems, Birkhauser, Berlin, Germany, pp 4-6, 33-48.

[7] Knobloch, H. W., Isidori, A., and Flockerzi, D. (1993). Topics in Control Theory, Birkhauser, Berlin, Germany, pp. 43-49, 58-67, 99-111.

[8] Liu, F., Ma, X., and Zhang, Z. (2014). Mu-Method for Robust Stability of Active Aeroelastic Wing with Multiple Control Surfaces, *Mechatronic and Automatic control systems, Lecture Notes in electrical Engineering*, Springer International publishing Switzerland.

[9] Pei, J., and Newsom, J. R. (2015). Robust Stability Analysis of the space Launch System Control Design: A Singular Value Approach, *AIAA paper*.

[10] Hjartarson, A., Seiler, P. J., and Balas, G. J. (2013). LPV Aeroservoelastic Control Using the LPV Tools Toolbox, *AIAA Atmospheric Flight Mechanics Conference*. doi:10.2514/6.2013-4742.

[11] Lee, K. W., and Singh, S.G. (2006). Global Robust Control of an Aeroelastic System Using Output Feedback, *AIAA Paper*.

[12] Julian, T., Harald, P., and Peter, S. (2015). Robust Control Design for Active Flutter Suppression, *AIAA paper*.

[13] Perry, B., and Cole, S. R. (1995). Summary of an Active Flexible Wing Program, *Journal of Aircraft*, Vol. 32, No. 1, pp. 10–15. doi:10.2514/3.46677

[14] Liebeck, R. H. (2004). Design of the Blended Wing Body Subsonic Transport, *Journal of Aircraft*, Vol. 41, No. 1, pp. 10–25. doi:10.2514/1.9084.

[15] Malecek, J. Cecrdle, J. Scotti, A. Ricci, S. Kiessling, F. and Klimmek, T. (2005). Dynamic Response Analysis and Experimental Validation of the X-DIA Demonstrator Component Model, Proceedings of the IFASD International Forum on Aeroelasticity, *International Forum on Aeroelasticity and Structural Dynamics*, Munich, Germany.

[16] Ricci, S. Scotti, A. Malecek, J. and Cecrdle, J. (2005). Experimental Investigations of a Vibration Suppression System for a Three Surface Aeroelastic Model, *Proceedings of the*

46th AIAA/ASME/ASCE/AHS/ ASC Structures, Structural Dynamics and Materials Conference, AIAA, Reston, VA, 18–21.

[17] De Gaspari, A. Ricci, S. Riccobene, L. and Scotti, A. (2009). Active Aeroelastic Control over a Multi Surface Wing: Modeling and Wind-Tunnel Testing, *AIAA Journal*, Vol. 47, No. 9.

[18] Dowell, E. H. (2015). A Modern Course in Aeroelasticity, Solid Mechanics and its Applications.
doi: 10.1007/978-3-319-09453-3_12.

COPYRIGHT STATEMENT